

Fire-retardant solid polymer electrolyte films prepared from oxetane derivative with dimethyl phosphate ester group

Ryo Shibutani and Hiromori Tsutsumi\*

Applied Molecular Bioscience, Graduate School of Medicine, Yamaguchi University,  
2-16-1, Tokiwa, Ube, 755-8611 Japan

Phone: +81-836-85-9282

Fax: +81-836-85-9201

E-mail: [tsutsumi@yamaguchi-u.ac.jp](mailto:tsutsumi@yamaguchi-u.ac.jp)

\*Corresponding author

## Abstract

Fire-retardant polymer electrolytes are key materials for safer operation of lithium secondary batteries and other large-size batteries than the batteries with organic liquid electrolyte. Solid polymer electrolyte systems with fire-retardant polymer matrixes have been investigated in only few cases. We prepare an oxetane derivative with dimethyl phosphate ester group (DPOX). The cross-linked poly(oxetane) matrixes for solid polymer electrolytes are prepared from DPOX and oxetane-based cross-linker (DDOE). DDOE has two oxetane rings at both of the ends of oligo-ethylene oxide chain. Conductivities in the range of  $10^{-5}$  S cm<sup>-1</sup> have been obtained for self-extinguishing, ion-conductive cross-linked poly(oxetane) matrix with DPOX and DDOE monomers. Polarization behavior of a lithium electrode in the cross-linked poly(oxetane)-based electrolyte films is also investigated. The polarization curves show some hysteresis character with potential steps, however, deposition and stripping of lithium on the lithium electrode are observed.

*Key words:* poly(oxetane), fire retardant, self-extinguishable polymer, lithium battery, solid polymer electrolyte

## 1. Introduction

Improvements in safety of lithium-ion and lithium batteries are very important to construct large-sized secondary batteries for electric vehicles and load leveling systems. Large-sized batteries have large amounts of electrolyte and active materials, anode and cathode. Non-flammability of the electrolyte in the large-sized batteries is an important point for their safe operation. To decrease flammability of the electrolyte systems the fire-retardant reagents are added into them. Organic phosphorous compounds have been used as additives for their flame-retardant properties [1]. Some organic phosphorous compounds, tris(2,2,2-trifluoroethyl) phosphite [2], trimethyl phosphite [3], dimethyl methyl phosphonate [4, 5], tributyl phosphate[6], triphenyl phosphate [6-8], tris(trifluoroethyl) phosphate [8], and cresyl diphenyl phosphate [9] were used as solvents or additives into the liquid electrolytes for lithium-ion and lithium batteries. Addition of the organic phosphorous compounds provides non-flammability of the electrolytes and affects battery performance, discharge capacity, life time, and so on. Some of them tent to decrease the overall efficiency of the battery systems.

Solid polymer electrolyte systems are promising candidates for construction of non-flammable batteries. Polymer is non-volatile and more stable thermally than normal organic solvents. Polymer electrolyte systems with fire retardant property have been investigated about poly(acrylonitrile)-based gel systems [10-12] or

poly(vinylidenefluoride-*co*-hexafluoropropylene)-based [13, 14] gel electrolyte systems with organic phosphorus compounds, and poly(ethylene oxide)-based electrolyte system mixed with middle molecular weight organic phosphate compound [15]. Solid polymer electrolyte systems prepared from fire retardant polymer matrix have been very few cases as far as we know.

Fig. 1 (a) shows the monomer structure, oxetane derivative with dimethyl phosphate group (DPOX). This molecule has two characteristic moieties. One is dimethyl phosphate group and another is oxetane ring. Its dimethyl phosphate group acts as a radical scavenger at the combustion reaction and a promoter of carbon char layers by dehydration reaction caused with phosphoric acid [1]. Oxetane ring structure provides us trimethylene oxide chains from ring-opening polymerization. The poly(trimethylene oxide) derivatives have flexible back bone and low glass transition temperature, like ethylene oxide-based polymer [16-22].

In this paper we report preparation of solvent-free cross-linked poly(oxetane)-based electrolyte films from photo-initiated polymerization of DPOX and DDOE monomer (in Fig. 1(b)), and their flammability and performance as solid polymer electrolytes, conductivity and polarization behavior of a lithium electrode.

## 2. Experimental

All reagents were used as received unless otherwise described. Cross-linking reagent, 1,

9-bis(3-ethyl-3-oxetanyl)-2, 5, 8-trioxanonane (DDOE, Fig. 1(b)) was prepared as the reported route in our previous papers [18-20].

### *2.1. Preparation of monomer*

Oxetane derivative, (DPOX, Fig. 1(a)) was prepared by coupling reaction between 3-ethyl-3-hydroxymethyloxetane (EHOX, Aldrich) and dimethylchlorophosphate (Aldrich). Typical preparation procedure of DPOX is as follows: EHOX (4.40 mL, 38.6 mmol) and *N*-methylimidazole (4.27 ml, 54.1 mmol, Tokyo Kasei) was dissolved into dichloromethane (50mL) in the three-necked flask (200mL) equipped with a reflux condenser and a dropping funnel. The dichloromethane solution (15ml) with dimethylchlorophosphate (5 ml, 46.4 mmol) was added into the dropping funnel. The dichloromethane solution in the funnel was added into the EHOX solution, slowly, to prevent the violent reaction. After addition of all of the dimethylchlorophosphate solution, the mixture was stirred at room temperature (about 298 K) for 24 h. The reaction mixture was added into the ice-cooled ammonium chloride saturated aqueous solution. The mixture was washed with water (100 mL, 3 times) to remove the water-soluble byproducts and the starting reagents. Some amount of magnesium sulfate added into the water-washed dichloromethane solution to remove water. The dichloromethane and unreacted materials in the dried solution was removed under reduced pressure (423 K, 133Pa). The structure and purity (over 98%) of residue was checked by <sup>1</sup>H NMR and FTIR

measurements. Yield: 7.1 g, 82%.

The structure of DPOX was confirmed  $^1\text{H}$ -NMR and FTIR measurements.

$^1\text{H}$  NMR ( $\text{CDCl}_3$ , ppm) 0.93 (3H, t,  $J=7.6$  Hz,  $\text{CH}_3\text{CH}_2-$ ), 1.78 (2H, q,  $J=7.6$  Hz,  $\text{CH}_3\text{CH}_2-$ ), 3.80 (6H, d,  $J=10.9$  Hz,  $\text{CH}_3\text{-O-P}$ ), 4.19 (2H, d,  $J=5.3$  Hz, C- $\text{CH}_2\text{-O-P}$ ), 4.45 (4H, dd,  $J=19.7$ , 5.9 Hz, O- $\text{CH}_2\text{-C}$  in oxetane ring)

FTIR (neat,  $\text{cm}^{-1}$ ) 848 (oxetane ring's C-O-C), 1273 ((RO)<sub>2</sub>PO), 2863, 2961 (CH<sub>2</sub>, CH<sub>3</sub>)

## 2. 2. Preparation of cross-linked electrolyte films by using cationic photo-initiator

The electrolyte films were prepared by photo-initiating cationic polymerization. We used diphenyliodonium hexafluorophosphate (DPIHFP, Tokyo Kasei) as a cationic photo-initiator. Typical preparation procedure is as follows: the mixture of DPOX (0.1726 g, 0.76 mmol), DDOE (0.2480 g, 0.78 mmol), LiBF<sub>4</sub> (0.0729 g, 0.77 mmol), and DPIHFP (0.0196 g, 0.05 mmol) was stirred at room temperature for 2 h in the dark. The resulted homogeneous solution was pored into an aluminum foil dish and then irradiated for 2 h at room temperature with a high-pressure mercury lamp (250 W, average energy was 12.78 J cm<sup>-2</sup>), (Optical Module X, USHIO). The resulted film was flexible and free-standing. Other electrolyte films were also prepared under similar procedure. The resulted electrolyte film is presented as (DPOX)1(DDOE)1(LiBF<sub>4</sub>)1 film. This means that the molar ratio of DPOX, DDOE, and LiBF<sub>4</sub> is 1: 1: 1. The electrolyte films containing other lithium salt, lithium

bis(trifluoromethanesulphonyl)imide (LiTFSI) was also prepared under similar procedure.

### *2. 3. Fire retardant test of samples*

Fire retardant test of the electrolyte films was performed with a Bunsen gas burner as an ignition source. A sample film (about 3 - 5 mm square) picked up with a pair of tweezers was set on the gas flame of the burner. The distance between sample film and the top of the flame of the gas burner was 2 cm. The period for the sample ignition ( $T_i$ ) was recorded. After the sample ignition, the ignition source was removed and the flame on the sample was timed until it self-extinguished.

### *2. 4. Measurements*

Infrared spectra of samples were recorded with an FTIR spectrophotometer (IRPresatge-21, Shimadzu).  $^1\text{H}$ -NMR spectra of the oxetane monomer were obtained on an NMR spectrophotometer (EX-270, JEOL). XRD patterns of the composites films were recorded with an X-ray diffraction meter (XD-D1, Shimadzu, CuK $\alpha$ ,  $\lambda=0.1542$  nm). DSC measurements of the samples were preformed with a differential scanning calorimeter (DSC5100S, Bruker AXS); heating rate was  $10 \text{ K min}^{-1}$ .

Conductivity of the prepared electrolyte films was measured by using an LCR meter. An electrolyte film was sandwiched with two stainless steel plates (13 mm in diameter).

Conductivity of the electrolyte film was measured with an LCR meter (HIOKI 3532-80 chemical impedance meter, 100 mV<sub>p-p</sub>, 10 - 100 kHz) under various temperature conditions from 293 K to 353 K.

Electrochemical characterization of the solid polymer electrolyte films was performed with polarization measurement of lithium electrode in the polymer electrolyte film. Detail cell configuration for electrochemical measurements was reported in our previous papers [21, 22].

Electrochemical measurements were performed with a computer-controlled potentiogalvanostat (HZ-5000, Hokuto Denko) under Ar atmosphere (dew point was at 203 K) at 328 K.

### 3. Results and discussion

#### *3.1. Fire retardant property of poly(oxetane)-based electrolyte films*

Structure of the poly(oxetane)-based electrolyte films prepared from DPOX and DDOE was confirmed from FTIR spectra of the films. Disappearance of the peaks attributed to the oxetane structure was established, which indicates that the oxetane rings in the monomers are opened by the photo-initiator. The resulted electrolyte films were flexible and free-standing. The XRD patterns of the poly(oxetane)-based films prepared from DPOX and DDOE with and without lithium salts had very broad peaks. The results suggest that the

poly(oxetane)-based films are amorphous and the polymer matrixes can dissolve the lithium salts in themselves. The glass transition temperature ( $T_g$ ) of the films is listed in Table 1. The  $T_g$  of (DPOX)1(DDOE)1 film (lithium salt-free film) is 248 K. Addition of LiBF<sub>4</sub> in the film elevated the  $T_g$  of the film to 277K. Addition of LiTFSI did not increase the  $T_g$  of the matrix, considerably. Thus, anion of lithium salt will affect the mobility of polymer chains in the oxetane-based matrix.

Flammability of the DPOX-based electrolyte film was compared with that of the DDOE-based film without DPOX, P(DDOE). The P(DDOE) film was prepared from DDOE (cross-linker) and DPIHFP (photo-initiator). Fig. 2 (a) shows the P(DDOE) film on the flame of the gas burner (the ignition source). After 4 s later, the sample ignited as shown Fig. 2 (b),  $T_i = 4$  s. Removing the ignition source did not affect the combustion status of the P(DDOE) film. After 10 s later, the P(DDOE) film burned away as shown in Fig 2 (c). The results suggest that the P(DDOE) film is flammable and not self-extinguishable.

The similar flammability test was applied to the (DPOX)1(DDOE)1(LiBF<sub>4</sub>)1 film. Fig. 2 (d) shows the (DPOX)1(DDOE)1(LiBF<sub>4</sub>)1 film on the flame of the ignition source. After 60 s later, the sample ignited as shown Fig. 2 (e),  $T_i = 60$  s. After removing the ignition source the flame on the film was immediately disappeared as shown in Fig 2 (f). This suggested that the (DPOX)1(DDOE)1(LiBF<sub>4</sub>)1 film is self-extinguishable. Char layer (containing carbonaceous compounds) was found on the surface of the self-extinguished film as shown in Fig. 2 (f). The

self-extinguishable property of the (DPOX)1(DDOE)1(LiBF<sub>4</sub>)1 is induced by the char production as similar fire-retardant mechanism of the organic phosphorous compounds [1]. Other cross-linked DPOX- and DDOE-based electrolytes with LiTFSI and without lithium salt also show similar fire retardant behavior and self-extinguishable property. The DPOX-based films have fire-retardant and self-extinguishable properties based on the DPOX unit with the alkyl phosphate group.

### *3.2. Conductivity of poly(oxetane)-based electrolyte films*

Temperature dependence of conductivity for poly(oxetane)-based electrolyte films are shown in Fig. 3. Conductivity of the lithium salt-free film (open triangle in Fig. 3) was 0.49  $\mu\text{S cm}^{-1}$  at 353 K. The charge carriers in the lithium ion-free film are produced by decomposition of the photo-initiator, DPIHFP. The estimated charge carriers from DPIHFP and its photo-reacted products are PF<sub>6</sub> anion, diphenyliodonium cation, phenyliodonium cation, and so on [23, 24]. Conductivity of the electrolyte films with lithium salt is one to three orders of magnitude higher than that of the lithium ion-free film. Conductivity at 353 K of the (DPOX)1(DDOE)1(LiX)n was 5.15  $\mu\text{S cm}^{-1}$  (X = BF<sub>4</sub>, n=1) and 56.1  $\mu\text{S cm}^{-1}$  (X = TFSI, n=1), and 0.122 mS cm<sup>-1</sup> (X = TFSI, n=2). The temperature dependence curves of conductivity for the electrolyte films are slightly convex. The curves are best fitted to an expression of the equation (1):

$$\sigma = A T^{-1/2} \exp [-B/R(T-T_0)] \quad (1)$$

where  $\sigma$  is conductivity,  $A$  is pre-exponential factor, which is proportional to the number of charge carriers,  $B$  is estimated activation energy for conduction,  $R$  is gas constant,  $T$  is absolute temperature, and  $T_0$  is normally called the equilibrium glass-transition temperature [25, 26].  $T_0$  is set for 50K lower than  $T_g$ . Fig. 4 shows the VTF plots for the electrolyte films and the lithium salt-free film. All plots show the linear relationships. The estimated parameters,  $A$  and  $B$ , are listed in Table 2. The estimated activation energy of the lithium salt-free film is  $7.14 \text{ kJ mol}^{-1}$  ( $0.074 \text{ eV}$ ). The  $A$  value of the film is  $0.003 \text{ Scm}^{-1} \text{ K}^{1/2}$ . The value is three orders of magnitudes smaller than that of the electrolyte films with LiTFSI salt. This indicates that the number of the charge carries in the lithium-ion free film is very low and the ions from the photo-initiator did not affect the conducting behavior of the DPOX and DDOE-based electrolyte films. The  $A$  value of the films with LiTFSI is larger than that with LiBF<sub>4</sub>. This suggests that dissolution ability of LiTFSI is larger than LiBF<sub>4</sub>. Higher glass transition temperature of the electrolyte film with LiBF<sub>4</sub> affects their lower conducting behaviors. The estimated activation energy of the DPOX-based electrolyte films is from  $6.52 \text{ kJ mol}^{-1}$  ( $0.068 \text{ eV}$ ) to  $9.51 \text{ kJ mol}^{-1}$  ( $0.099 \text{ eV}$ ). These values are similar to other systems' values; the PEO-based electrolytes with PC or EC as a plasticizer ( $0.058 - 0.082 \text{ eV}$ ) [27] ,

PEG-LiClO<sub>4</sub> system with alumina nano-particles (0.09 - 0.12 eV) [28], PEO-LiCF<sub>3</sub>SO<sub>3</sub> systems (0.090 - 0.125 eV) [29]. The conduction mechanism of the cross-linked DPOX- and DDOE-based electrolyte films is similar to those of the other electrolyte systems. Dissolution support groups in the cross-linked DPOX- and DDOE-based electrolyte systems are the oligo-ethylene oxide chains in the DDOE monomer, dimethyl phosphate group in the DPOX, and trimethylene oxide chain prepared from ring-opening polymerization of oxetane rings in DPOX and DDOE. The trimethylene oxide chains and oligo-ethylene oxide chains support the migration of ions in the matrix prepared from DPOX and DDOE.

### *3.3. Polarization behavior of lithium electrode in the electrolyte films with dimethyl phosphate ester group*

Fig. 5 shows the polarization curves of a lithium electrode in the (DPOX)1(DDOE)1(LiTFSI)n, (n = 1 or 2) electrolyte films at 328 K. The polarization behaviors indicated that deposition and stripping of lithium on the lithium electrode occurred in the poly(oxetane)-based electrolyte films [21, 22]. However, the polarization curves of lithium electrode in the DPOX-based electrolyte film gave asymmetrical forms, which is fairly different from those observed in liquid electrolytes [30]. The cathodic limiting current of lithium in (DPOX)1(DDOE)1(LiTFSI)2 electrolyte was much lower than that for anodic polarization and for cathodic polarization in (DPOX)1(DDOE)1(LiTFSI)1 electrolyte film.

The reason is not clear. Decrease in concentration of lithium ions at the lithium/(DPOX)1(DDOE)1(LiTFSI)2 interface under the highly cathodic polarized condition may be induced this phenomenon. Trapping of lithium ions by the phosphate groups in the side chains may affect mobility of lithium ions in the (DPOX)-based matrix.

## Conclusion

We prepared the fire-retardant solid polymer electrolytes from the oxetane derivative with dimethyl phosphate ester group (DPOX). The fire retardant and self-extinguishable properties of the DPOX-based electrolyte films are induced from the alkyl phosphate structure as similar fire-retardant mechanism by organic phosphate compounds, which form char layer on the surface of the materials. Conductivity of the DPOX-based electrolyte films is in the range from  $5.15 \mu\text{S cm}^{-1}$  to  $0.122 \text{ mS cm}^{-1}$  at 353 K. Temperature dependence of conductivity is VTF-type one. The estimated activation energy of conduction is in the range from  $6.52 \text{ kJ mol}^{-1}$  ( $0.068 \text{ eV}$ ) to  $9.51 \text{ kJ mol}^{-1}$  ( $0.099 \text{ eV}$ ). Polarization behavior of lithium electrode in the DPOX-based electrolyte shows asymmetrical forms, which is fairly different from those observed in liquid electrolytes. Current hysteresis, especially, at cathodic polarization is also observed.

## Acknowledgements

This work was partially financial supported by Grant-in-Aid for Scientific Research (C),  
KAKENHI (21560883) and Electric technology research foundation of Chugoku.

## References

- [1] F. Laoutid, L. Bonnaud, M. Alexandre, J.M. Lopez-Cuesta, P. Dubois, Materials Science and Engineering: R: Reports, 63 (2009) 100-125.
- [2] S.S. Zhang, K. Xu, T.R. Jow, Journal of Power Sources, 113 (2003) 166-172.
- [3] X.L. Yao, S. Xie, C.H. Chen, Q.S. Wang, J.H. Sun, Y.L. Li, S.X. Lu, Journal of Power Sources, 144 (2005) 170-175.
- [4] J.K. Feng, X.P. Ai, Y.L. Cao, H.X. Yang, Journal of Power Sources, 177 (2008) 194-198.
- [5] H.F. Xiang, H.Y. Xu, Z.Z. Wang, C.H. Chen, Journal of Power Sources, 173 (2007) 562-564.
- [6] Y.E. Hyung, D.R. Vissers, K. Amine, Journal of Power Sources, 119-121 (2003) 383-387.
- [7] E.G. Shim, T.H. Nam, J.G. Kim, H.S. Kim, S.I. Moon, Journal of Power Sources, 172 (2007) 919-924.
- [8] D.H. Doughty, E.P. Roth, C.C. Crafts, G. Nagasubramanian, G. Henriksen, K. Amine, Journal of Power Sources, 146 (2005) 116-120.
- [9] Q. Wang, P. Ping, J. Sun, C. Chen, Journal of Power Sources, 196 (2011) 5960-5965.
- [10] H. Akashi, K. Sekai, K.I. Tanaka, Electrochimica Acta, 43 (1998) 1193-1197.

- [11] H. Akashi, K.I. Tanaka, K. Sekai, Journal of Power Sources, 104 (2002) 241-247.
- [12] H. Akashi, K.I. Tanaka, K. Sekai, Journal of the Electrochemical Society, 145 (1998) 881-887.
- [13] B.S. Lalia, T. Fujita, N. Yoshimoto, M. Egashira, M. Morita, Journal of Power Sources, 186 (2009) 211-215.
- [14] M. Morita, Y. Niida, N. Yoshimoto, K. Adachi, Journal of Power Sources, 146 (2005) 427-430.
- [15] Y. Li, H. Zhan, L. Wu, Z. Li, Y. Zhou, Solid State Ionics, 177 (2006) 1179-1183.
- [16] J.B. Kerr, G. Liu, L.A. Curtiss, P.C. Redfern, Electrochimica Acta, 48 (2003) 2305-2309.
- [17] G. Liu, C.L. Reeder, X. Sun, J.B. Kerr, Solid State Ionics, 175 (2004) 781-783.
- [18] Y. Miwa, H. Tsutsumi, T. Oishi, Polymer Journal, 33 (2001) 568-574.
- [19] Y. Miwa, H. Tsutsumi, T. Oishi, Polymer Journal, 33 (2001) 927-933.
- [20] Y. Miwa, H. Tsutsumi, T. Oishi, Electrochemistry, 70 (2002) 264-269.
- [21] Y. Shintani, H. Tsutsumi, Journal of Power Sources, 195 (2010) 2863-2869.
- [22] Y. Shintani, H. Tsutsumi, Electrochemistry, 78 (2010) 387-389.
- [23] J.V. Crivello, Polymer, 46 (2005) 12109-12117.
- [24] J.V. Crivello, B. Falk, M.R. Zonca, Journal of Polymer Science Part A:

Polymer Chemistry, 42 (2004) 1630-1646.

[25] P.G. Bruce, F.M. Gray, 6. Polymer electrolytes II: Physical principles, in: P.G. Bruce (Ed.) Solid state electrochemistry, Cambridge university press, 1995, pp. 119-162.

[26] M.A. Ratner, P. Johansson, D.F. Shriver, MRS Bulletin, 25 (2000) 31-37.

[27] Y.-J. Wang, Y. Pan, D. Kim, Polymer International, 56 (2007) 381-388.

[28] T.J. Singh, S.V. Bhat, Journal of Power Sources, 129 (2004) 280-287.

[29] N.K. Karan, D.K. Pradhan, R. Thomas, B. Natesan, R.S. Katiyar, Solid State Ionics, 179 (2008) 689-696.

[30] Y. Matsuda, M. Morita, H. Tsutsumi, Journal of Power Sources, 44 (1993) 439-443.

## Figure captions

Fig. 1 Structures of oxetane derivatives, (a) DPOX and (b) DDOE (cross-linker).

Fig. 2 Flammability test of samples, P(DDOE) matrix, (a) 0 s, (b) 4 s (ignition of sample) and (c) 10s (burn out of sample), and (DPOX)1(DDOE)1(LiBF<sub>4</sub>)1 electrolyte film, (d) 0 s, (e) 60 s (ignition of sample), and (f) self-extinguished sample film.

Fig. 3 Temperature dependence of conductivity of the cross-linked poly(oxetane)-based electrolyte films. Closed circle (DPOX)1(DDOE)1(LiTFSI)2, open circle (DPOX)1(DDOE)1(LiTFSI)1, closed square (DPOX)1(DDOE)1(LiBF<sub>4</sub>)1, and open triangle (DPOX)1(DDOE)1 matrix.

Fig. 4 VTF-plots of the cross-linked poly(oxetane)-based electrolyte films. Closed circle (DPOX)1(DDOE)1(LiTFSI)2, open circle (DPOX)1(DDOE)1(LiTFSI)1, closed square (DPOX)1(DDOE)1(LiBF<sub>4</sub>)1, and open triangle (DPOX)1(DDOE)1 matrix.

Fig. 5 Polarization curves of lithium electrode in the solid polymer electrolyte, closed circle (DPOX)1(DDOE)1(LiTFSI)2, open circle (DPOX)1(DDOE)1(LiTFSI)1.

Table 1 Glass transition temperature of (DPOX)1(DDOE)1(X)n films

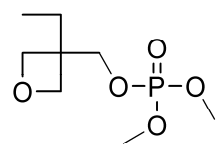
X	n	$T_g$ / K
-	-	248
LiBF <sub>4</sub>	1	277
LiTFSI	1	256
LiTFSI	2	251

Table 2 VTF parameters of (DPOX)1(DDOE)1(X)n electrolyte films <sup>a)</sup>

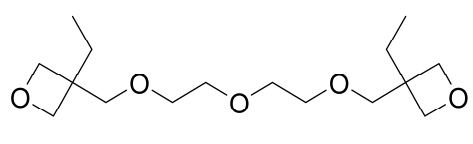
X	n	A (S cm <sup>-1</sup> K <sup>1/2</sup> )	B (kJ mol <sup>-1</sup> )	B (eV)
-	-	0.003	7.14	0.074
LiBF <sub>4</sub>	1	0.042	6.52	0.068
LiTFSI	1	2.21	9.39	0.097
LiTFSI	2	4.24	9.51	0.099

a)  $T_0 = T_g - 50$

Fig. 1



(a)



(b)

Fig. 2 (a)

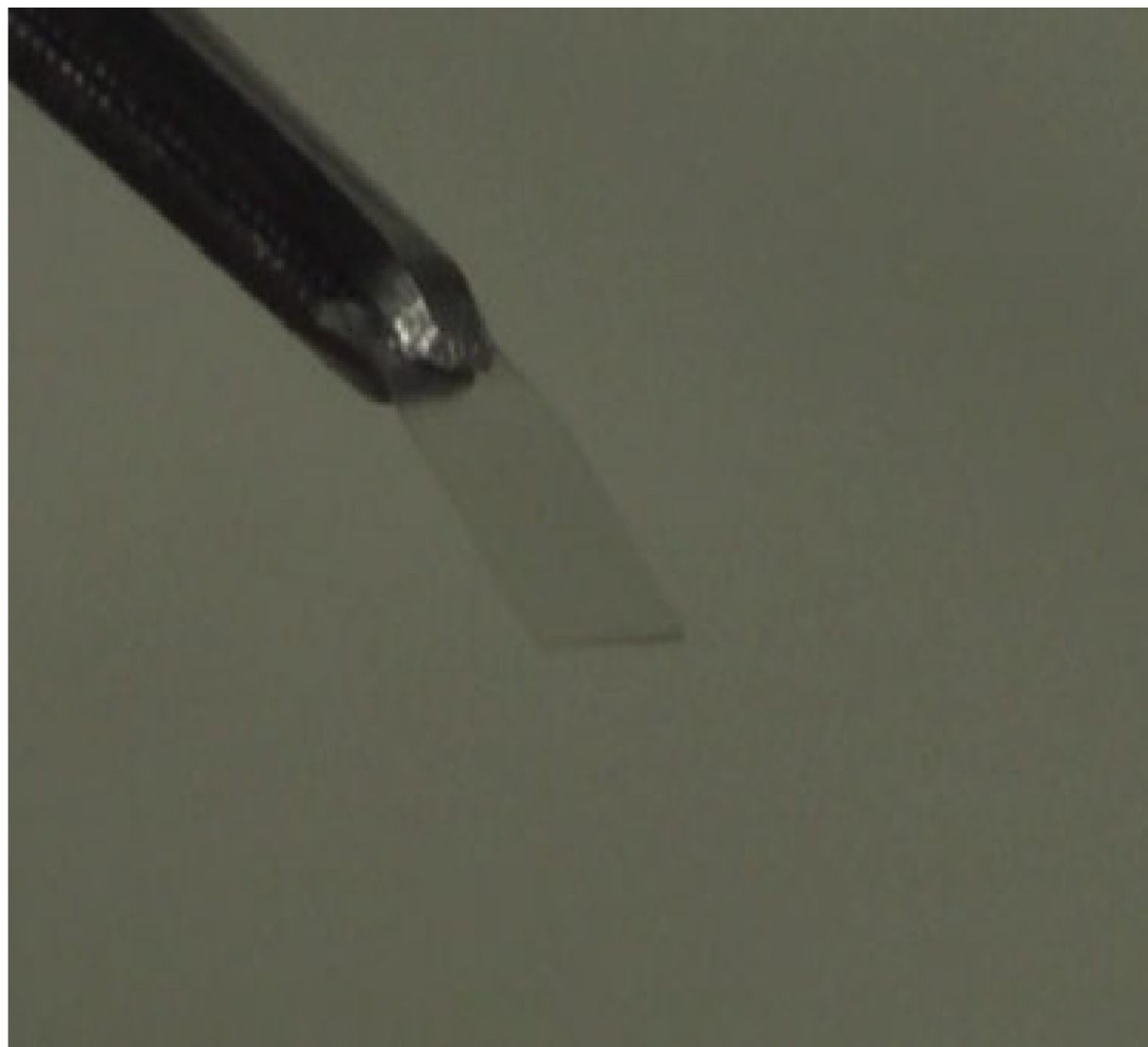


Fig.2 (b)

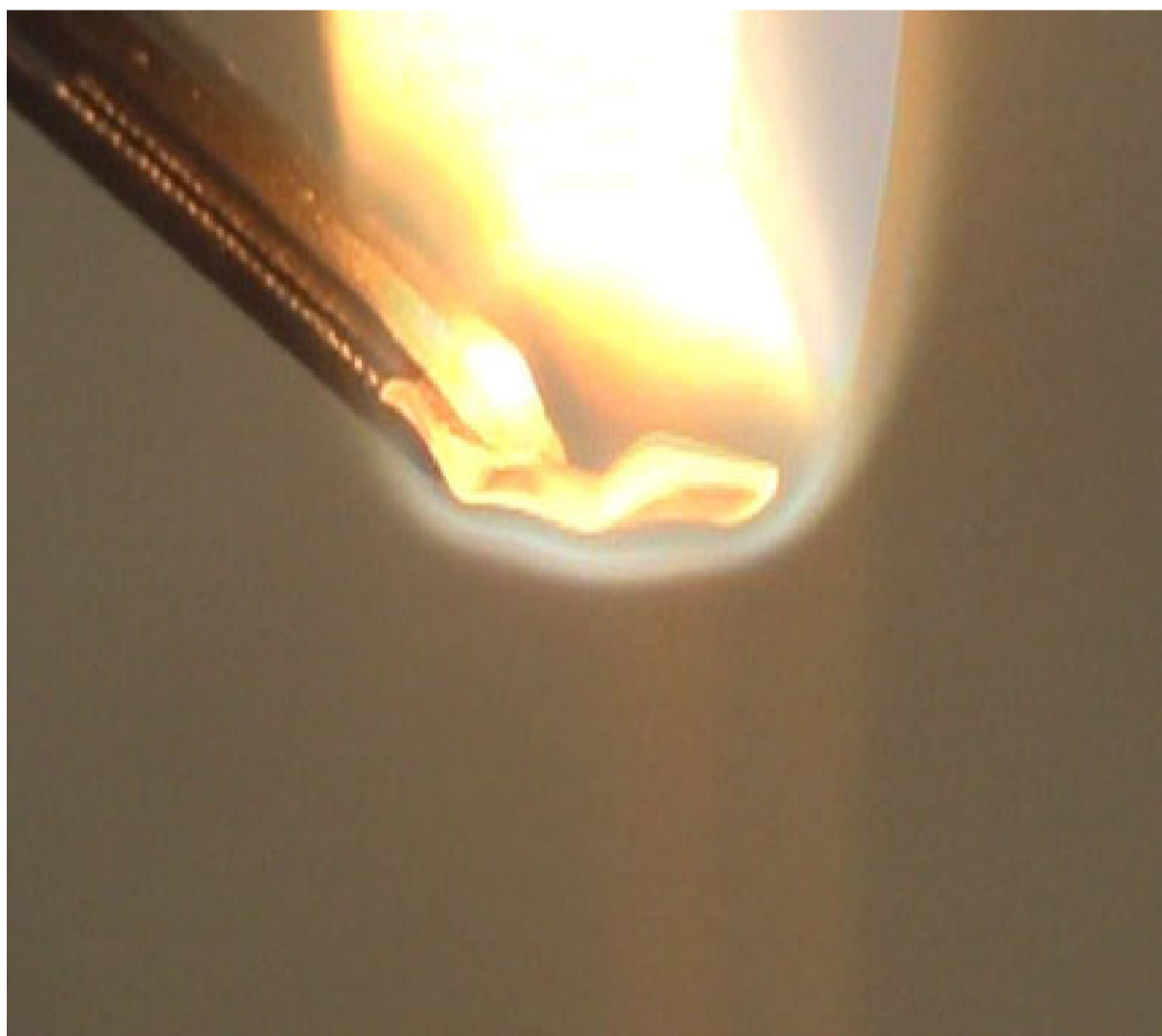


Fig. 2 (c)

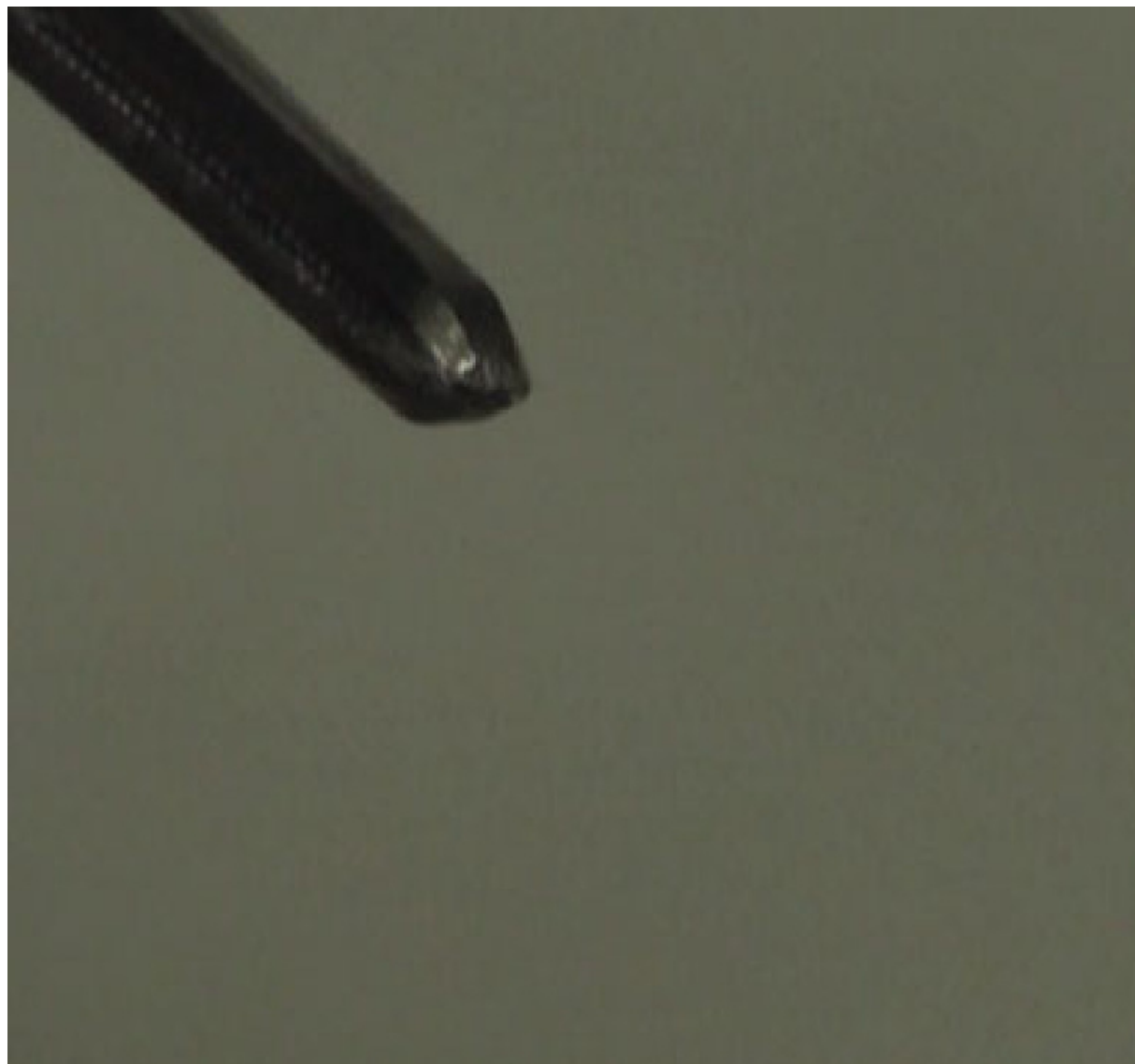


Fig. 2 (d)

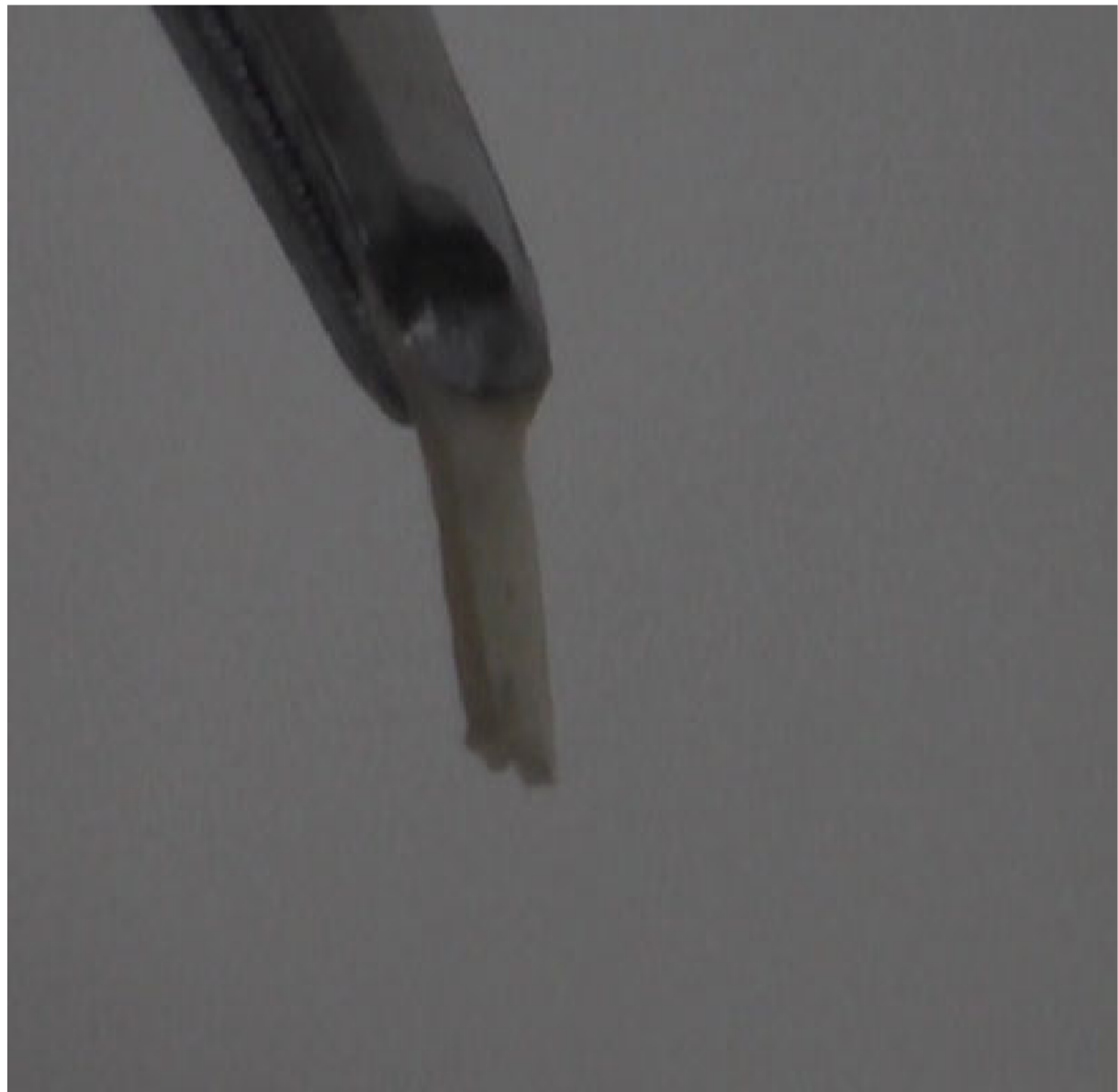


Fig. 2 (e)



Fig. 2 (f)

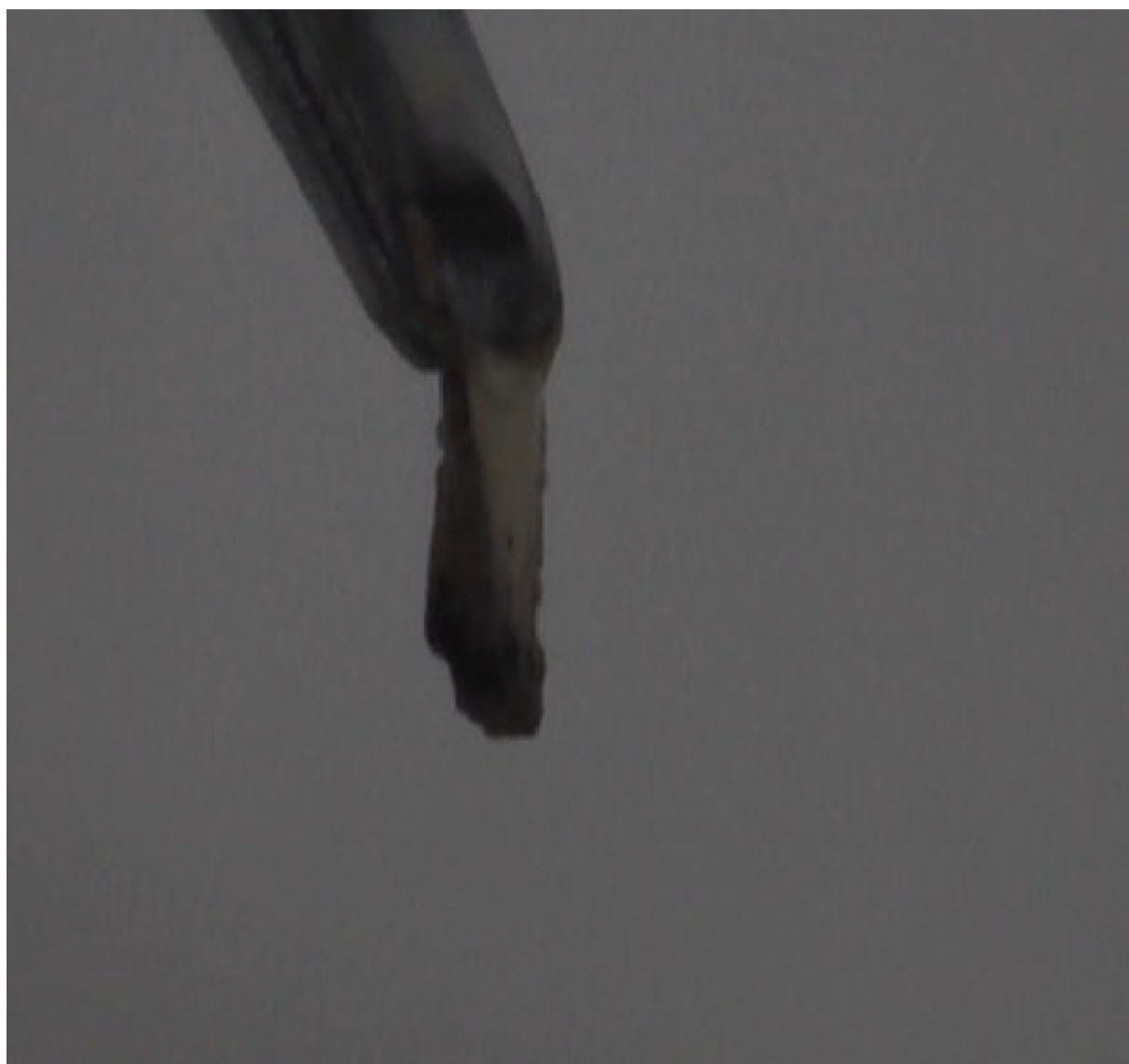


Fig. 3

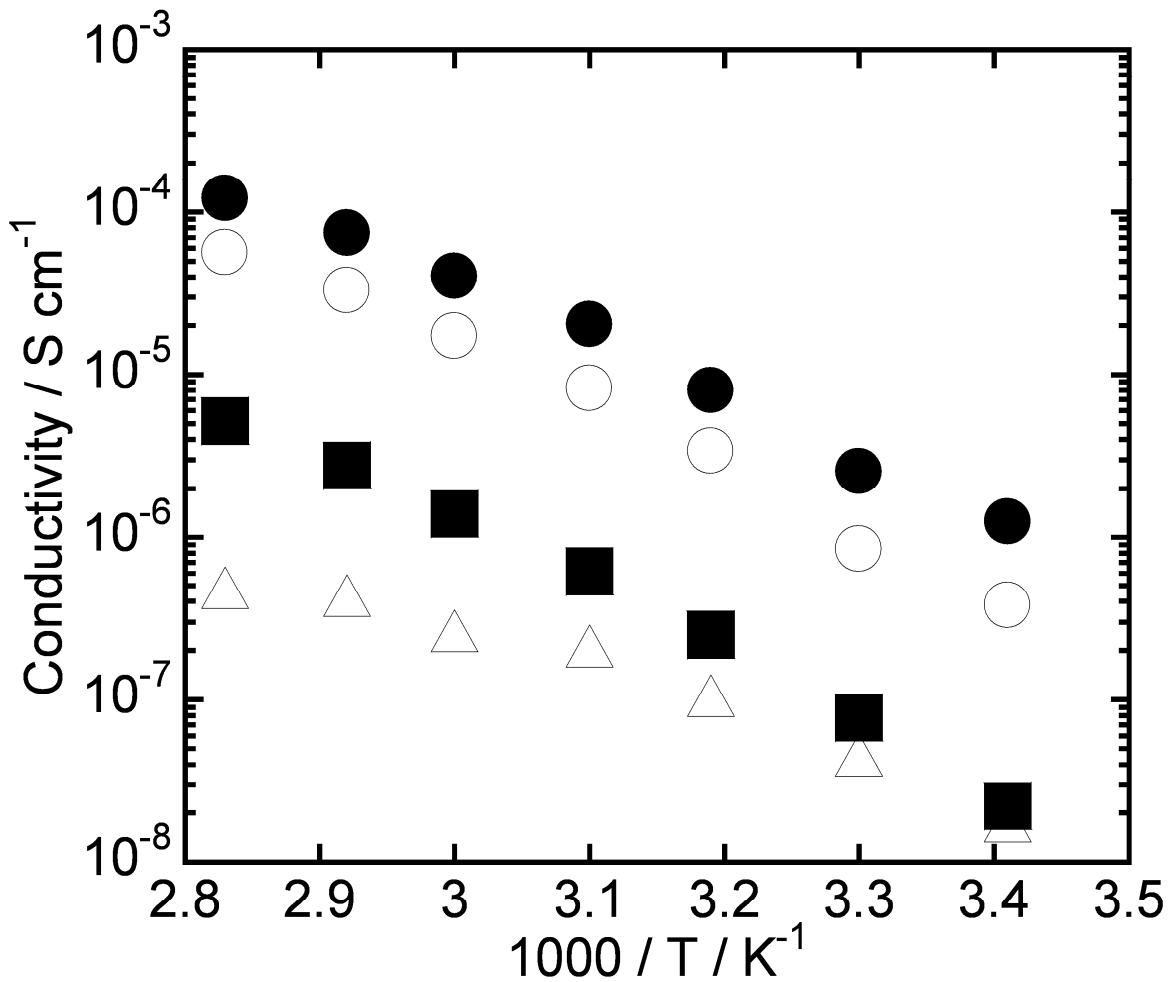


Fig. 4

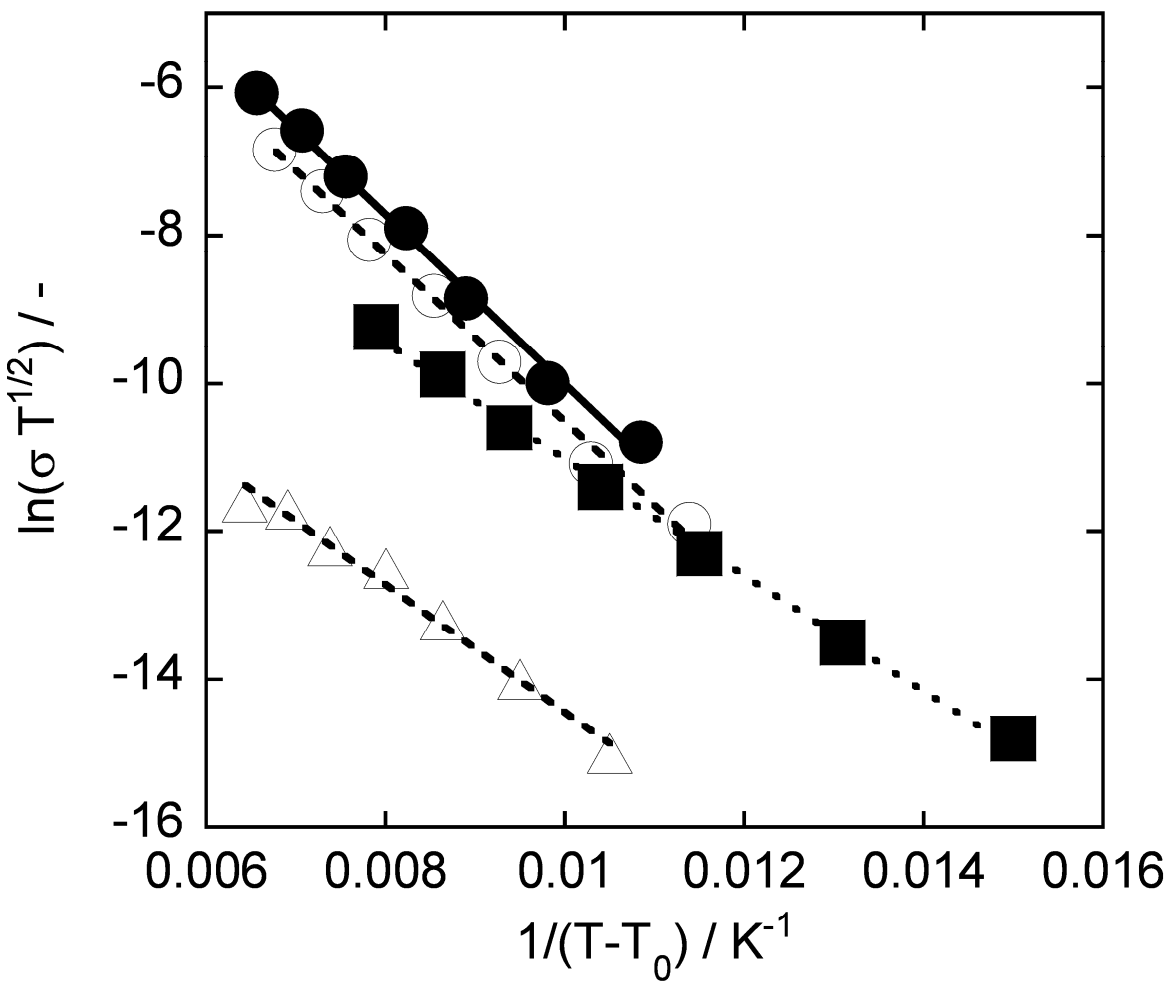


Fig. 5

